Kamenevite, $K_2TiSi_3O_9 \cdot H_2O$, a new mineral with microporous titanosilicate framework from the Khibiny alkaline complex, Kola peninsula, Russia

Igor V. PEKOV[1,2,*], Natalia V. ZUBKOVA[1], Vasiliy O. YAPASKURT[1], Dmitry I. BELAKOVSKIY[3], Inna S. LYKOVA[1], Sergey N. BRITVIN[4], Anna G. TURCHKOVA[1] and Dmitry Y. PUSHCHAROVSKY[1]

[1]Faculty of Geology, Moscow State University, Vorobievy Gory, 119991 Moscow, Russia
*Corresponding author, e-mail: igorpekov@mail.ru
[2]Vernadsky Institute of Geochemistry and Analytical Chemistry, Russian Academy of Sciences, Kosygina str. 19, 119991 Moscow, Russia
[3]Fersman Mineralogical Museum of Russian Academy of Sciences, Leninsky Prospekt 18-2, 119071 Moscow, Russia
[4]Department of Crystallography, St Petersburg State University, Universitetskaya Nab. 7/9, 199034 St. Petersburg, Russia

Abstract: The new zeolite-like titanosilicate mineral kamenevite $K_2TiSi_3O_9 \cdot H_2O$, isostructural with umbite $K_2ZrSi_3O_9 \cdot H_2O$, is found in two peralkaline pegmatites located at Mt. Suoluaiv (Oleniy Ruchey mine: holotype) and Mt. Rasvumchorr (Rasvumchorr mine) in the Khibiny alkaline complex, Kola peninsula, Russia. It is a hydrothermal mineral associated with lomonosovite, aegirine, villiaumite, pectolite, shafranovskite, ershovite, umbite, potassic feldspar, sodalite, lamprophyllite, *etc.* Kamenevite occurs as lamellar crystals up to $0.02 \times 0.1 \times 0.3$ mm and their aggregates up to 0.7 mm (Oleniy Ruchey) or grains up to 0.15 mm across (Rasvumchorr). The mineral is transparent, colourless (white in aggregates), with vitreous lustre. It is brittle, the Mohs hardness is *ca.* 4. Cleavage is (010) good. $D_{meas} = 2.69(2)$, $D_{calc} = 2.698$ g cm^{-3}. Kamenevite is optically biaxial (–), $\alpha = 1.650(4)$, $\beta = 1.678(5)$, $\gamma = 1.685(5)$, $2V_{meas} = 60(10)°$. The chemical composition of the holotype [wt%, electron microprobe data, H_2O content calculated for 1 (H_2O) *pfu*] is: $Na_2O = 0.48$, $K_2O = 24.37$, $CaO = 0.13$, $Fe_2O_3 = 0.35$, $SiO_2 = 48.78$, $TiO_2 = 20.30$, $ZrO_2 = 0.89$, $Nb_2O_5 = 0.35$, $H_2O = 4.85$, total = 100.50. The empirical formula calculated on the basis of 10 O atoms per formula unit (*apfu*) is $(K_{1.92}Na_{0.06}Ca_{0.01})_{\Sigma1.99}(Ti_{0.94}Zr_{0.03}Fe_{0.02}Nb_{0.01})_{\Sigma1.00}S_{3.01}O_9 \cdot H_2O$. Kamenevite is orthorhombic, $P2_12_12_1$, $a = 9.9166(4)$, $b = 12.9561(5)$, $c = 7.1374(3)$ Å, $V = 917.02(6)$ Å^3 and $Z = 4$. The strongest reflections of the powder XRD pattern [d,Å(I)(hkl)] are: 7.92(70)(110), 6.51(47)(020), 5.823(95)(101), 2.988(84)(301, 122), 2.954(100)(041, 320), 2.906(68)(311, 202) and 2.834(69)(141, 212). The crystal structure (single-crystal XRD data, $R = 0.0384$) is based on a microporous heteropolyhedral framework built by $[Si_3O_9]^\infty$ wollastonite-type chains linked by isolated Ti-centred octahedra. The K^+ cations and H_2O molecules are located in wide and narrower [001] channels. The mineral is named in honour of the outstanding Russian geologist Evgeniy Arsenievich Kamenev (1934–2017) who made great contribution to the geology of the Khibiny complex.

Key-words: kamenevite; new mineral; umbite; crystal structure; microporous titanosilicate; mixed framework; peralkaline pegmatite; Khibiny alkaline complex; Kola peninsula.

1. Introduction

One of the bright and specific features of derivatives of peralkaline magmatic rocks is the great diversity of minerals with topologically various microporous structures which possess zeolitic properties. Besides aluminosilicate zeolites and pyrochlore-like oxides, there are numerous zeolite-like titano-, niobo- or zirconosilicates with structures based on heteropolyhedral frameworks consisting of corner-sharing tetrahedra SiO_4 and octahedra MO_6, where M = Ti, Nb or Zr. Similarly to zeolites, their structures contain voluminous cages and systems of crossing wide channels in which large cations and/or H_2O molecules occur (Sandomirsky & Belov, 1984; Chukanov & Pekov, 2005; Krivovichev, 2005). Almost all such zeolite-like minerals are endemics

of the peralkaline formation and crystallize mainly in pegmatites and hydrothermal bodies related to agpaitic rocks (Pekov & Chukanov, 2005). Many of these minerals have analogues or close relatives among synthetic microporous silicates with mixed heteropolyhedral frameworks which have been the focus of active studies during the last three decades, due to their strong and selective ion-exchange, molecular-sieve, catalytic and other technologically important properties (Bortun *et al.*, 1999; Saxton, 1999; Clearfield, 2000; Kuznicki *et al.*, 2001; *etc.*). However, the known diversity of titano-, niobo- or zirconosilicate minerals is much greater than the diversity of related synthetic phases. This fact makes peralkaline pegmatites and hydrothermal bodies a unique source of very helpful information on crystal chemistry and physico-chemical

conditions of formation and transformations of these compounds.

Microporous, zeolite-like titanosilicates with heteropolyhedral Ti–Si–O frameworks compose the largest family among the above-mentioned minerals and this family continues to increase. The present paper describes a new hydrous potassium titanosilicate from peralkaline pegmatites of the famous Khibiny alkaline complex at Kola peninsula. This mineral species was named kamenevite (Cyrillic: каменевит) in honour of the outstanding Russian geologist Evgeniy Arsenievich Kamenev (1934–2017), who made great contribution to the geology of the Khibiny complex and its mineral deposits (Zak *et al.*, 1972; Kamenev, 1974, 1975; Kamenev & Mineev, 1982). Dr. Kamenev is one of the discoverers of the Oleniy Ruchey apatite deposit, the holotype locality of the new mineral.

Both the new mineral and its name have been approved by the IMA Commission on New Minerals, Nomenclature and Classification (IMA 2017-021). The type specimen is deposited in the systematic collection of the Fersman Mineralogical Museum of the Russian Academy of Sciences, Moscow, with the catalogue number 95903.

2. Occurrence and general appearance

Specimens with the new mineral were found by the authors (IVP and ISL) in potassium-rich peralkaline (hyperagpaitic) pegmatites related to rischorrites that are associated with apatite–nepheline rocks at two apatite deposits within the Khibiny complex.

The holotype material was collected in June 2016 in dumps of the Oleniy Ruchey (Reindeer Stream) underground mine at Mt. Suoluaiv in the south-east part of the Khibiny Mountains. This mine operates the Oleniy Ruchey apatite deposit. The pegmatite was found in several lumps. It is mainly composed by potassic feldspar, nepheline, sodalite, aegirine, alkali amphibole of the arfvedsonite series, lamprophyllite, lomonosovite, and eudialyte; the accessory minerals belonging to the early, properly pegmatitic assemblage are shcherbakovite, sphalerite, galena, and molybdenite. In some areas of the pegmatite enriched in green acicular aegirine, there are nests of hydrothermal minerals consisting mainly of pectolite, villiaumite, ershovite, and shafranovskite. Umbite, kamenevite, sidorenkite, djerfisherite, rasvumite, and Na-bearing neotocite are observed in minor amounts. Kamenevite replaces lomonosovite and fills cracks in crystals of slightly etched lomonosovite (Fig. 1). The new mineral occurs as coarse lamellar crystals up to $0.02 \times 0.1 \times 0.3$ mm, rectangular (Fig. 2) or irregular in shape, flattened on [010]. The major crystal form is pinacoid {010}, lateral faces are probably pinacoids {100} and {001}. Crystals are combined in aggregates up to 0.7 mm across.

In August 2017 kamenevite was determined in a similar mineral assemblage in a pegmatite found in dumps from the level +470 m of the Rasvumchorr underground apatite mine situated at Mt. Rasvumchorr, in the south part of Khibiny. The major constituents of the pegmatite are potassic feldspar, nepheline, sodalite, Na–Mg–Fe^{3+}-enriched hedenbergite, aegirine, potassic-arfvedsonite,
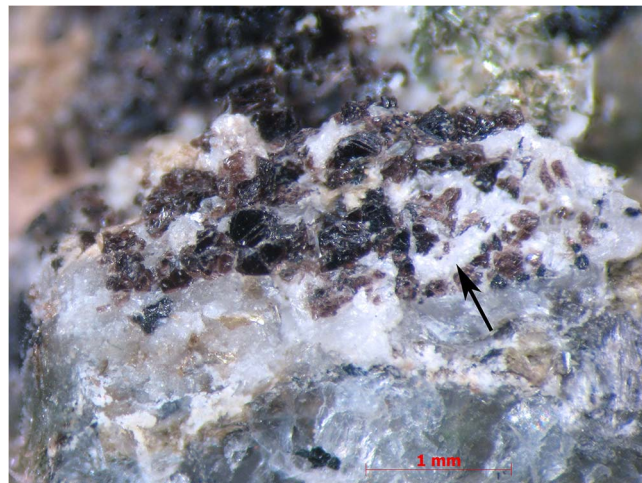

Fig. 1. White aggregates of kamenevite (marked with arrow) replacing brown to brown-black lomonosovite in a pegmatite mainly consisting of colourless potassic feldspar, with subordinate green aegirine and yellow lamprophyllite. The holotype specimen of kamenevite from Oleniy Ruchey. Field of view: 4.4 mm. Photo: I.V. Pekov & A.V. Kasatkin.
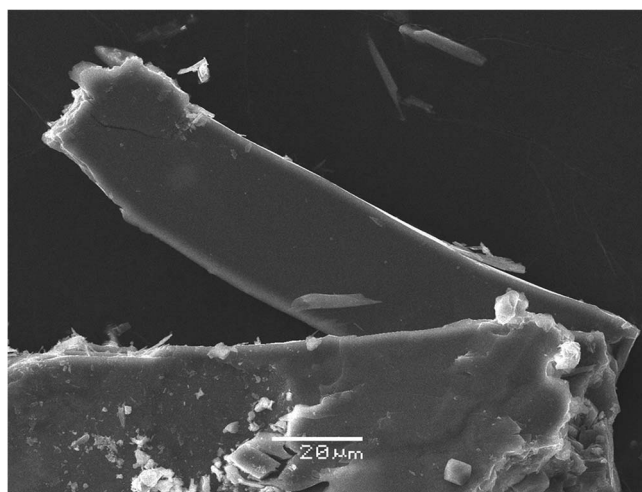

Fig. 2. Crystal of kamenevite from Oleniy Ruchey. SEM (BSE) image.

lamprophyllite, eudialyte, and lomonosovite; subordinate and accessory pegmatitic minerals are annite, fluorapatite, shcherbakovite, lobanovite, sphalerite, galena, and molybdenite. Sporadically the pegmatite contains abundant and unusually diverse (especially in part of potassium-rich silicates and sulfides) hydrothermal mineralization forming lenticular or irregular in shape nests up to 20 cm across: there are pectolite, natrolite, villiaumite, lovozerite-group minerals, shafranovskite, zakharovite, ershovite (and highly hydrated products of its alteration), paraershovite, tinaksite, phosinaite-(Ce), umbite, kamenevite, tiettaite, lithosite, barytolamprophyllite, chkalovite, loparite, nacaphite, natrophosphate, K-rich vishnevite, cryptophyllite, shlykovite, mountainite, fluorapophyllite-(K), neotocite, cobaltite, djerfisherite, chlorbartonite, and rasvumite. Kamenevite

occurs as equant or flattened grains up to 0.15 mm across, sometimes cavernous, and granular accumulations up to 0.1×0.4 mm embedded in aggregates of different hydrous silicates. The new mineral is closely associated with shafranovskite, altered ershovite and lovozerite (Fig. 3).

3. Physical properties and optical data

Kamenevite is transparent, colourless in small individuals and white in aggregates, with a white streak and a vitreous lustre. The mineral is brittle, with a Mohs hardness of *ca.* 4. Good cleavage on (010) was observed under the scanning electron microscope. The fracture is stepped. Density measured by flotation in heavy liquids (bromoform + dimethylformamide) is 2.69(2), and the density calculated using the empirical formula and single-crystal unit-cell parameters is 2.698 g cm^{-3} (both values are for the holotype).

Kamenevite is optically biaxial (–), refraction indices for the holotype are: $\alpha = 1.650(4)$, $\beta = 1.678(5)$, $\gamma = 1.685(5)$ (589 nm), with $2V$ (meas.) $= 60(10)°$, $2V$ (calc.) $= 52°$. Under the microscope the mineral is colourless and non-pleochroic. Dispersion of optical axes was not observed. Orientation: $Y = b$.

4. Chemical composition

The chemical composition of kamenevite was studied using a Jeol JSM-6480LV scanning electron microscope equipped with an INCA-Wave 500 wavelength-dispersive spectrometer (Laboratory of Analytical Techniques of High Spatial Resolution, Dept. of Petrology, Moscow State University), with an acceleration voltage of 20 kV, a beam current of 20 nA and a beam diameter of 3 μm. The following standards were used: NaCl (Na), microcline (K), CaMoO₄ (Ca), Y (Y), Mn (Mn), FeAsS (Fe), diopside (Si), Ti (Ti), Zr (Zr), Nb (Nb). Contents of other elements with atomic numbers higher than carbon are below detection limits.

H₂O was not analysed because of the paucity of material. The water content was calculated based on the crystal-structure data (see below) showing the presence of 1 H₂O molecule *pfu*. The calculated values for samples from both localities demonstrate a good agreement with the analytical totals derived from the constituents measured using the electron microprobe. The correctness of the calculation is also confirmed by very low Gladstone-Dale compatibility index values (Mandarino, 1981) for the holotype: $1 - (K_p/K_c) = -0.001$ if D (meas.) is used, or 0.002 if D (calc.) is used, both *superior*.

The chemical composition of kamenevite and, for comparison, its isostructural Zr-dominant analogue umbite from the same localities, is given in Table 1.

The empirical formula of the holotype calculated on the basis of 10 O *apfu* [= O₉(H₂O)] is $(K_{1.92}Na_{0.06}Ca_{0.01})_{\Sigma1.99}$ $(Ti_{0.94}Zr_{0.03}Fe_{0.02}Nb_{0.01})_{\Sigma1.00}S_{3.01}O_9 \cdot H_2O$. The end-member formula of kamenevite is $K_2TiSi_3O_9 \cdot H_2O$.

The holotype specimen from Oleniy Ruchey is closer chemically to the end-member than samples from Rasvumchorr, which contain distinct admixtures of zirconium (up to 2.2 wt% ZrO₂ = 0.07 Zr *pfu*), iron (up to
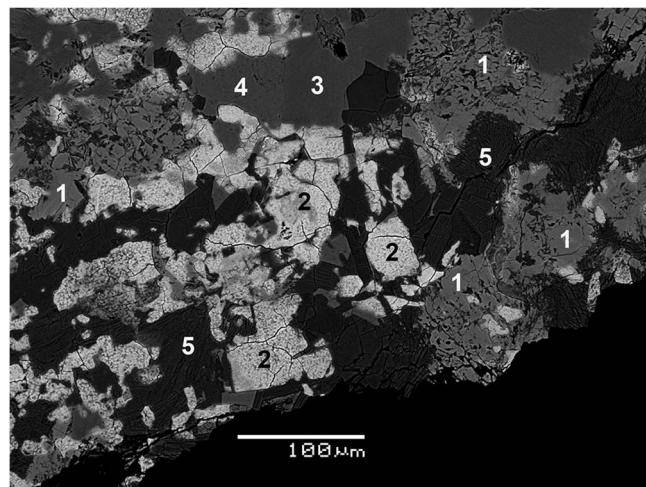

Fig. 3. Grains and aggregates of kamenevite (1) within a nest consisting of lovozerite (2), pectolite (3), shafranovskite (4) and altered ershovite (5). Sample from Mt. Rasvumchorr. SEM (BSE) image.

1.0 wt% Fe₂O₃ = 0.05 Fe *pfu*) and sodium (up to 1.2 wt% Na₂O = 0.14 Na *pfu*) (Table 1).

5. X-ray crystallography and crystal structure

Powder X-ray diffraction (XRD) data of kamenevite from both localities were collected with a Rigaku R-AXIS Rapid II single-crystal diffractometer equipped with cylindrical image plate detector (radius 127.4 mm) using Debye-Scherrer geometry, Co $K\alpha$ radiation (rotating anode with VariMAX microfocus optics), 40 kV, 15 mA, and 15 min exposure. Angular resolution of the detector is 0.045 2θ (pixel size 0.1 mm). The data were integrated using the software package Osc2Tab (Britvin *et al.*, 2017). Powder XRD data for the holotype are given in Table S1 (deposited in Supplementary Material linked to this article and freely available on the GSW website of the journal: https://pubs.geoscienceworld.org/eurjmin).

The orthorhombic unit-cell parameters calculated from the powder data are (holotype sample from Oleniy Ruchey/sample from Rasvumchorr): $a = 9.924(3)/9.933(4)$, $b = 12.964(3)/12.965(5)$, $c = 7.150(2)/7.123$ (4) Å and $V = 919.9(7)/917(1)$ Å^3.

Single-crystal X-ray diffraction study of the holotype sample of kamenevite was carried out using an Xcalibur S diffractometer equipped with a CCD detector. More than a hemisphere of three-dimensional data was collected. Crystal data, data collection information and structure refinement details are given in Table 2. Data reduction was performed using CrysAlisPro Version 1.171.37.34 (Agilent Technologies, 2014). The data were corrected for Lorentz and polarization effects. Empirical absorption correction using spherical harmonics, implemented in SCALE3 ABSPACK scaling algorithm, was applied. The structure was solved by direct methods and refined with the use of SHELX software package (Sheldrick, 2008) on the basis of 2201 independent reflections with $I > 2\sigma(I)$ to the final $R = 0.0384$.

Table 1. Chemical composition of kamenevite (1–4) and associated umbite (5–6).

No.	1	2	3	4	5	6
			wt%			
Na_2O	0.48 (0.21–0.69)	0.38	1.19		1.12	1.84
K_2O	24.37 (24.11–24.53)	24.57	23.36	25.30	21.73	19.96
CaO	0.13 (0.10–0.16)	0.10	0.28		0.27	0.26
MnO	bdl	0.08	0.12		bdl	0.29
Fe_2O_3*	0.35 (0.13–0.52)	0.30	1.01		0.62	2.87
Y_2O_3	bdl	bdl	bdl		bdl	0.30
SiO_2	48.78 (47.19–50.29)	47.19	47.92	48.40	45.58	44.86
TiO_2	20.30 (19.75–20.66)	19.67	19.40	21.46	4.82	0.83
ZrO_2	0.89 (0.41–1.83)	2.17	1.30		22.11	24.16
Nb_2O_5	0.35 (0.00–0.63)	0.19	0.48		bdl	0.49
H_2O_{calc}**	4.85	4.75	4.81	4.84	4.53	4.45
Total	100.50	99.40	99.87	100.00	100.85	100.31
		Formula calculated on the basis of 10 O *apfu* [= $O_9(H_2O)$]				
Na	0.06	0.05	0.14		0.14	0.24
K	1.92	1.97	1.86	2	1.83	1.72
Ca	0.01	0.01	0.02		0.02	0.02
Y	–	–	–		–	0.01
Mn	–	0.00	0.01		–	0.02
Fe	0.02	0.01	0.05		0.03	0.15
Ti	0.94	0.93	0.91	1	0.24	0.04
Zr	0.03	0.07	0.04		0.71	0.79
Nb	0.01	0.01	0.01		–	0.01
Si	3.01	2.97	2.99	3	3.02	3.02
ΣA	*1.99*	*2.03*	*2.02*	*2*	*1.99*	*1.99*
ΣM	*1.00*	*1.02*	*1.02*	*1*	*0.98*	*1.01*

Note: 1, 5 – Oleniy Ruchey (1 – the holotype sample of kamenevite: average for four analyses, ranges are in parentheses), 2, 3, 6 – Rasvumchorr, 4 – calculated values for $K_2TiSi_3O_9·H_2O$; bdl – below detection limit; ΣA = Na + K+Ca + Y, ΣM = Mn + Fe + Ti + Zr + Nb; *Fe is calculated as Fe^{3+} because of its presence as admixture in the site with strong predominance of a high-valence constituent, Ti^{4+} or Zr^{4+}; **calculated by stoichiometry, for 1 H_2O molecule *pfu*.

Table 2. Crystal data, data collection information and structure refinement details for kamenevite.

Formula	$K_2TiSi_3O_9·H_2O$
Formula weight	372.39
Temperature, K	293(2)
Radiation and wavelength, Å	Mo $K\alpha$; 0.71073
Crystal system, space group, Z	Orthorhombic, $P2_12_12_1$, 4
Unit-cell dimensions, Å	a = 9.9166(4)
	b = 12.9561(5)
	c = 7.1374(3)
V, Å³	917.02(6)
Absorption coefficient μ, mm⁻¹	2.275
F_{000}	736
Crystal size, mm	0.01 × 0.06 × 0.10
Diffractometer	Xcalibur S CCD
θ range for data collection, °	3.26 – 30.75
Reflections collected	8359
Independent reflections	2590 (R_{int} = 0.0515)
Independent reflections, $I > 2\sigma(I)$	2201
Data reduction	CrysAlisPro, ver. 1.171.37.34 (Agilent Technologies, 2014)
Absorption correction	multi-scan
Structure solution	direct methods
Refinement method	full-matrix least-squares on F^2
Number of refined parameters	153
Final R indices [$I > 2\sigma(I)$]	$R1$ = 0.0384, w$R2$ = 0.0783
R indices (all data)	$R1$ = 0.0521, w$R2$ = 0.0835
GoF	1.026
Largest diff. peak and hole, e/Å³	0.81 and −0.48

Table 3. Atom coordinates and thermal displacement parameters (U_{eq}, in Å²) for kamenevite.

Site	x	y	z	U_{eq}
Ti	0.45402(6)	0.21149(5)	0.25896(9)	0.00875(13)
Si(1)	0.17925(10)	0.17337(8)	0.00725(14)	0.0107(2)
Si(2)	0.03799(10)	0.04663(8)	0.73134(14)	0.0102(2)
Si(3)	0.64289(10)	0.33164(8)	0.58120(14)	0.0106(2)
K(1)	0.20601(11)	0.63449(9)	0.15160(18)	0.0353(3)
K(2)	0.43286(10)	0.07911(8)	0.70532(13)	0.0264(2)
O(1)	0.4246(3)	0.3641(2)	0.2444(4)	0.0142(5)
O(2)	0.3362(3)	0.1908(2)	0.0496(3)	0.0139(6)
O(3)	0.5138(3)	0.0684(2)	0.2711(4)	0.0142(5)
O(4)	0.5598(3)	0.2388(2)	0.4894(4)	0.0147(6)
O(5)	0.6137(3)	0.2300(2)	0.1015(4)	0.0147(6)
O(6)	0.3025(3)	0.1895(2)	0.4276(4)	0.0136(6)
O(7)	0.0964(3)	0.1497(2)	0.2015(4)	0.0179(6)
O(8)	0.1014(3)	0.0590(2)	0.5198(4)	0.0149(6)
O(9)	0.1628(3)	0.0708(2)	0.8769(4)	0.0162(6)
Ow	0.6825(4)	0.0655(3)	0.8764(6)	0.0377(9)
H(1)	0.748(3)	0.096(4)	0.825(6)	0.032(15)*
H(2)	0.656(6)	0.108(4)	0.960(7)	0.07(2)*

*U_{iso}.

Positions of hydrogen atoms were found in a difference Fourier map and refined in a semi-free way: Ow–H distances were restrained to 0.85(1) Å. Atom coordinates and displacement parameters are presented in Table 3 and 4, selected

Table 4. Anisotropic displacement parameters (in Å^2) for kamenevite.

Site	U_{11}	U_{22}	U_{33}	U_{23}	U_{13}	U_{12}
Ti	0.0092(3)	0.0101(3)	0.0069(3)	0.0000(2)	−0.0006(3)	−0.0007(2)
Si(1)	0.0116(5)	0.0131(5)	0.0075(4)	0.0003(4)	−0.0017(4)	0.0000(4)
Si(2)	0.0115(4)	0.0105(4)	0.0085(4)	−0.0004(4)	−0.0002(4)	0.0000(4)
Si(3)	0.0100(4)	0.0139(5)	0.0079(4)	0.0004(4)	−0.0007(4)	−0.0006(4)
K(1)	0.0312(6)	0.0268(5)	0.0478(7)	0.0089(5)	−0.0107(5)	−0.0091(5)
K(2)	0.0263(5)	0.0269(5)	0.0262(5)	0.0092(4)	0.0018(4)	0.0023(4)
O(1)	0.0118(12)	0.0140(12)	0.0167(13)	0.0006(11)	−0.0020(12)	−0.0007(10)
O(2)	0.0134(13)	0.0163(15)	0.0119(13)	−0.0009(10)	−0.0007(10)	−0.0011(11)
O(3)	0.0162(12)	0.0105(12)	0.0159(13)	0.0006(11)	−0.0012(10)	0.0003(10)
O(4)	0.0143(13)	0.0178(15)	0.0120(12)	0.0011(10)	−0.0043(11)	−0.0009(12)
O(5)	0.0148(13)	0.0113(14)	0.0180(14)	0.0007(11)	0.0039(11)	0.0019(11)
O(6)	0.0113(12)	0.0202(16)	0.0093(12)	−0.0023(11)	0.0007(10)	0.0005(12)
O(7)	0.0145(12)	0.0311(17)	0.0081(12)	0.0017(11)	0.0003(11)	−0.0067(12)
O(8)	0.0204(14)	0.0125(14)	0.0119(13)	−0.0006(10)	0.0058(11)	−0.0005(12)
O(9)	0.0154(13)	0.0149(14)	0.0183(14)	−0.0046(11)	−0.0071(11)	0.0027(12)
Ow	0.0294(19)	0.030(2)	0.053(3)	−0.0160(18)	0.0170(18)	−0.0062(17)

interatomic distances in Table 5, H-bond geometry in Table 6 and bond valence calculations in Table 7.

The crystal structure of kamenevite (Fig. 4a), as well as of its synthetic end-member analogue K$_2$TiSi$_3$O$_9$·H$_2$O (Lin *et al.*, 1997; Zou & Dadachov, 2000), is based on the heteropolyhedral framework built by [Si$_3$O$_9$]$^\infty$ wollastonite-type chains (Fig. 4b) linked by isolated Ti-centred octahedra. Each TiO$_6$ octahedron shares all six oxygen vertices with SiO$_4$ tetrahedra. The heteropolyhedral framework contains wide (approximate size 4.4 × 8.2 Å) and narrower (approximate size 3.1 × 5.2 Å) channels with elliptical cross-section running along [001] in which extra-framework K$^+$ cations (they occupy two crystallographically non-equivalent sites) and H$_2$O molecules are located. The K(1) sites and water molecules occupy the wider channels while K(2) sites are located in the narrower ones. The K(1) atom is surrounded by five oxygen atoms with distances in the range 2.609(4) to 2.960(3) Å and also forms four elongated K(1)–O bonds with distances varying from 3.182(3) to 3.427(3) Å. The K(2) atom is surrounded by six oxygen atoms with distances in the range 2.765(3) to 2.979(3) Å and three oxygen atoms with K(2)–O distances exceeding 3.0 Å: from 3.008(3) to 3.204(3) Å.

6. Discussion

Kamenevite is isostructural to umbite, K$_2$ZrSi$_3$O$_9$·H$_2$O (Ilyushin *et al.*, 1981; Khomyakov *et al.*, 1983; Ilyushin, 1993), with Ti instead of Zr (Table 8). The complete solid-solution series between the umbite-type K$_2$ZrSi$_3$O$_9$·H$_2$O and K$_2$TiSi$_3$O$_9$·H$_2$O was synthesized (Clearfield *et al.*, 1998; Lin *et al.*, 1999), but in nature this series demonstrates a significant gap as intermediate compositions close to the midpoint were not found yet. The highest Ti content in umbite was found by us in a sample from Oleniy Ruchey: 4.9 wt% TiO$_2$ which corresponds to 0.24 Ti *apfu* (Table 1, #5). In kamenevite the admixture of ZrO$_2$ reaches 2.2 wt% = 0.07 Zr *apfu* (sample from Rasvumchorr: Table 1, #2). Umbite and kamenevite were found in both

Table 5. Selected interatomic distances (Å) in the structure of kamenevite.

Ti – O(2)	1.916(3)	K(1) – Ow	2.609(4)
–O(6)	1.946(3)	–O(6)	2.787(3)
–O(3)	1.948(3)	–O(5)	2.799(3)
–O(5)	1.956(3)	–O(4)	2.869(3)
–O(4)	1.983(3)	–O(3)	2.960(3)
–O(1)	2.001(3)	–O(1)	3.182(3)
<Ti–O>	1.958	–O(7)	3.183(3)
		–O(4)	3.315(3)
Si(1)–O(2)	1.601(3)	–O(8)	3.427(3)
–O(5)	1.610(3)		
–O(9)	1.631(3)	K(2)–O(6)	2.765(3)
–O(7)	1.640(3)	–Ow	2.765(4)
<Si(1)–O>	1.621	–O(4)	2.871(3)
		–O(8)	2.890(3)
Si(2)–O(3)	1.602(3)	–O(9)	2.947(3)
–O(1)	1.622(3)	–O(7)	2.979(3)
–O(8)	1.643(3)	–O(2)	3.008(3)
–O(9)	1.646(3)	–O(9)	3.188(3)
<Si(2)–O>	1.628	–O(3)	3.204(3)
Si(3)–O(4)	1.598(3)		
–O(6)	1.608(3)		
–O(7)	1.636(3)		
–O(8)	1.643(3)		
<Si(3)–O>	1.621		

Table 6. Hydrogen-bond geometry (Å, °) in the structure of kamenevite.

D – H⋯A	D–H	H⋯A	D⋯A	$\angle(D – H⋯A)$
Ow – H(1)⋯O(1)	0.852(10)	1.886(18)	2.710(4)	162(5)
Ow – H(2)⋯O(5)	0.848(10)	1.93(2)	2.754(4)	165(7)

pegmatites described above but these minerals are not intimately associated; in both cases umbite is a constituent of pseudomorphs after eudialyte.

Table 7. Bond valence calculations* for kamenevite.

	Ti	Si(1)	Si(2)	Si(3)	K(1)	K(2)	Σ	H-bonding	Σ
O(1)	0.60		1.01		0.06		1.67	+0.22 (Ow)	1.89
O(2)	0.76	1.06				0.09	1.91		1.91
O(3)	0.70		1.06		0.11	0.05	1.92		1.92
O(4)	0.64			1.07	0.14	0.13	2.02		2.02
					0.04				
O(5)	0.68	1.04			0.16		1.88	+0.20 (Ow)	2.08
O(6)	0.70			1.04	0.17	0.18	2.09		2.09
O(7)		0.96		0.97	0.06	0.10	2.09		2.09
O(8)			0.95	0.95	0.03	0.13	2.06		2.06
O(9)		0.98	0.94			0.11	2.09		2.09
						0.06			
Ow = H₂O					0.27	0.18	0.45	−0.22 (O(1))	0.03
								−0.20 (O(5))	
Σ	4.08	4.04	3.96	4.03	1.04	1.03			

*Bond-valence parameters for Ti–O, Si–O and K–O pairs were taken from Brese & O'Keeffe (1991) and for H-bonding from Ferraris & Ivaldi (1988).

The synthetic counterpart of kamenevite known as *titanosilicate AM-2*, $K_2TiSi_3O_9 \cdot H_2O$, is in the focus of studies in applied chemistry because of its strong zeolitic properties. The synthesis, crystal structure, ion exchange and dehydration reactions for this compound were reported, as well as the crystal-chemistry of its ion-exchanged forms (Lin *et al.*, 1997; Valtchev *et al.*, 1999; Bortun *et al.*, 2000; Zou & Dadachov, 2000; Doebelin & Armbruster, 2007). It is worthy to note that the bond distances to the H_2O molecules are significantly different for the two K sites [*e.g.*, K(1) is more strongly bonded to H_2O than to the framework oxygen atoms] in kamenevite, its synthetic analogue and umbite.

Kamenevite demonstrates quite a rare case for minerals: it is a titanosilicate with a heteropolyhedral Ti–Si–O framework containing isolated TiO_6 octahedra. This structural feature is very common for ZrO_6 octahedra in microporous zirconosilicates with heteropolyhedral Zr–Si–O frameworks, unlike titano- or niobosilicates in which TiO_6 or NbO_6 octahedra usually form condensed motifs, typically chains with shared oxygen vertices, Ti/Nb–O–Ti/Nb bridges (Pyatenko *et al.*, 1999). This explains, *e.g.*, the rarity of titanium minerals belonging to the eudialyte, lovozerite, benitoite and hilairite groups in comparison to zirconium members of these groups, in spite of the significant prevalence of Ti over Zr in alkaline rocks and in Earth's crust in general (Pekov, 2005). The umbite–kamenevite pair is in a good agreement with this empirical regularity: umbite is a common late-stage mineral in Khibiny, typical product of the eudialyte hydrothermal alteration, whereas kamenevite has been found only in minor amounts in two pegmatites.

Kamenevite is a hydrothermal mineral formed at a late stage of the evolution of hyperagpaitic pegmatites, as a result of the influence of K-rich solutions (fluids). At Oleniy Ruchey it is a product of the hydrothermal alteration of lomonosovite, $Na_{10}Ti_4(Si_2O_7)_2(PO_4)_2O_4$, whereas at Rasvumchorr the new mineral probably crystallized directly from a hydrothermal solution.
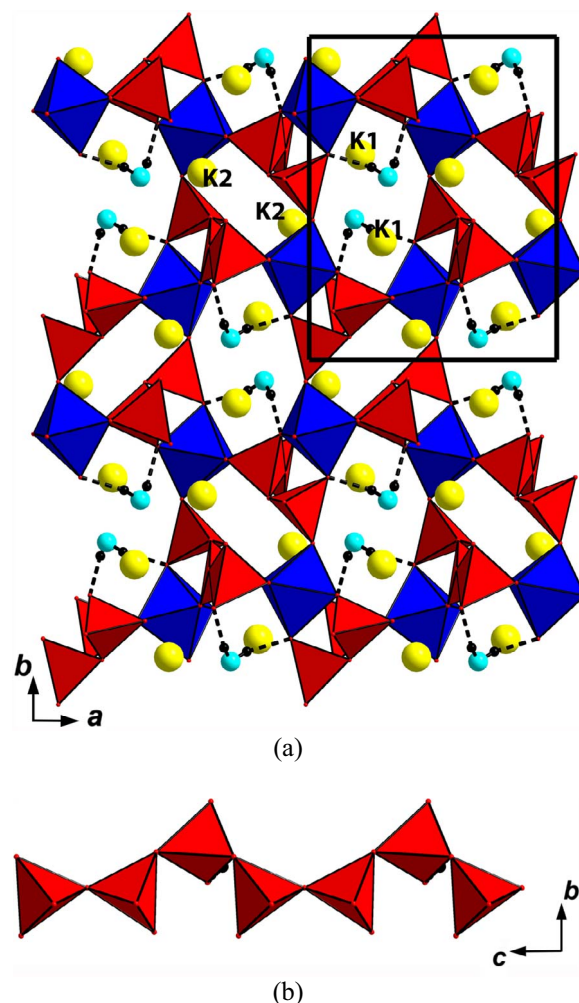

Fig. 4. The crystal structure of kamenevite in the *ab* projection (a, with outlined unit cell) and the wollastonite-type chain of SiO_4 tetrahedra in it (b). TiO_6 octahedra are deep blue, SiO_4 tetrahedra are red, K atoms are yellow circles, O atoms of H_2O molecules are light blue circles and H atoms are small black circles. Hydrogen bonds are shown as dashed lines.

Table 8. Comparative data of kamenevite and umbite.

Mineral	Kamenevite	Umbite
Formula	K$_2$TiSi$_3$O$_9$·H$_2$O	K$_2$ZrSi$_3$O$_9$·H$_2$O
Crystal system	Orthorhombic	Orthorhombic
Space group	$P2_12_12_1$	$P2_12_12_1$
a, Å	9.9166(4)	10.208(2)
b, Å	12.9561(5)	13.241(4)
c, Å	7.1374(3)	7.174(1)
V, Å^3	917.02(6)	970
Z	4	4
Strongest reflections of the	7.92–70	8.12–30
powder X-ray diffraction	6.51–47	6.56–60
pattern: d, Å – I	5.823–95	5.91–90
	3.462–36	3.59–30
	3.213–38	3.31–70
	2.988–84	3.02–100
	2.954–100	2.87–80
	2.906–68	2.156–40
	2.834–69	1.797–80
Optical data	1.650(1)	1.596(2)
α	1.678(5)	1.610 (calc.)
β	1.685(5)	1.619(2)
γ	(–) 60°	(–) 80°
Optical sign, 2V (meas.)	1.650(1)	1.596(2)
Density (meas.), g cm^{-3}	2.69	2.79
Density (calc.), g cm^{-3}	2.698	2.79
Source	this work	Khomyakov *et al.*, 1983; Ilyushin, 1993

References

Agilent Technologies (2014): CrysAlisPro Software system, version 1.171.37.34. Agilent Technologies UK Ltd, Oxford, UK.

Bortun, A.I., Bortun, L.N., Khainakov, S.A., Clearfield, A., Trobajo, C., Garcia, J.R. (1999): Hydrothermal synthesis and ion exchange properties of the novel framework sodium and potassium niobium silicates. *Solvent Extr. Ion Exch.*, **17**, 649–675.

Bortun, A.I., Bortun, L.N., Poojary, D.M., Xiang, O.-Y., Clearfield, A. (2000): Synthesis, characterization, and ion exchange behaviour of a framework potassium titanium trisilicate K$_2$TiSi$_3$O$_9$·H$_2$O and its protonated phases. *Chem. Mater.*, **12**, 294–305.

Brese, N.E. & O'Keeffe, M. (1991): Bond-valence parameters for solids. *Acta Crystallogr.*, **B47**, 192–197.

Britvin, S.N., Dolivo-Dobrovolsky, D.V., Krzhizhanovskaya, M.G. (2017): Software for processing the X-ray powder diffraction data obtained from the curved image plate detector of Rigaku RAXIS Rapid II diffractometer. *Zap. Ross. Mineral. Obshch.*, **146**, 104–107 (in Russian).

Chukanov, N.V. & Pekov, I.V. (2005): Heterosilicates with tetrahedral-octahedral frameworks: mineralogical and crystal-chemical aspects. *in* ''Micro- and Mesoporous Mineral Phases''. *Rev. Mineral. Geochem.*, **57**, 105–143.

Clearfield, A. (2000): Structure and ion exchange properties of tunnel type titanium silicates. *Solid State Sci.*, **3**, 103–112.

Clearfield, A., Bortun, A.I., Poojary, D.M., Khainakov, S.A., Bortun, L.N. (1998): On the selectivity regulation of K$_2$ZrSi$_3$O$_9$·H$_2$O-type ion exchangers. *J. Molec. Struct.*, **470**, 207–213.

Doebelin, N. & Armbruster, T. (2007): Microporous titanosilicate AM-2: Rb-exchange and thermal behaviour. *Mater. Res. Bull.*, **42**, 113–125.

Ferraris, G. & Ivaldi, G. (1988): Bond valence *vs* bond length in O···O hydrogen bonds. *Acta Crystallogr.*, **B44**, 341–344.

Ilyushin, G.D. (1993): New data on crystal structure of umbite K$_2$ZrSi$_3$O$_9$·H$_2$O. *Inorg. Mater.*, **27**, 1128–1133.

Ilyushin, G.D., Pudovkina, Z.V., Voronkov, A.A., Khomyakov, A.P., Ilyukhin, V.V., Pyatenko, Yu.A. (1981): The crystal structure of a new natural modification of K$_2$ZrSi$_3$O$_9$·H$_2$O. *Dokl. Akad. Nauk SSSR,* **257**, 608–610 (in Russian).

Kamenev, E.A. (1974): Structural zonation of Khibiny apatite deposits and prediction of hidden ore resources. *in* ''State and Perspective of Increase of Mineral-Resource Base of Russian North-West'', Nedra, Leningrad, 197–201 (in Russian).

— (1975): Geology and Structure of the Koashva Apatite Deposit, Leningrad, Nedra, 128 p. (in Russian).

Kamenev, E.A. & Mineev, D.A. (1982): New Khibiny Apatite Deposits. Nedra, Moscow, 182 p. (in Russian).

Khomyakov, A.P., Voronkov, A.A., Kobyashev, Yu.S., Polezhaeva, L.I. (1983): Umbite and paraumbite, new potassium zirconosilicates from the Khibiny alkaline massif. *Zap. Vses. Mineral. Obshch.,* **112**, 462–469 (in Russian).

Krivovichev, S.V. (2005): Topology of microporous structures. *in* ''Micro- and Mesoporous Mineral Phases'', *Rev. Mineral. Geochem.*, **57**, 17–68.

Kuznicki, S.M., Bell, V.A., Nair, S., Hillhouse, H.W., Jacubinas, R.M., Braunbarth, C.M., Toby, B.Y., Tsapatsis, M. (2001): A titanosilicate molecular sieve with adjustable pores for size-selective adsorption of molecules. *Nature*, **412**, 720–724.

Lin, Z., Rocha, J., Brandão, P., Ferreira, A., Esculcas, A. P., Pedrosa de Jesus, J. D., Philippou, A., Anderson, M.W. (1997): Synthesis and structural characterization of microporous umbite, penkvilksite, and other titanosilicates, *J. Phys. Chem. B,* **101**, 7114–7120.

Lin, Z., Rocha, J., Ferreira, P., Thursfield, A., Agger, J.R., Anderson, M.W. (1999): Synthesis and structural characterization of microporous framework zirconium silicates. *J. Phys. Chem. B,* **103**, 957–963.

Mandarino, J.A. (1981): The Gladstone-Dale relationship. Part IV. The compatibility concept and its application. *Can. Mineral.*, **14**, 498–502.

Pekov, I.V. (2005): Genetic Mineralogy and Crystal Chemistry of Rare Elements in Highly Alkaline Natural Systems. Dr. of Sciences Dissertation, Lomonosov Moscow State University, Moscow, 652 p. (in Russian).

Pekov, I.V. & Chukanov, N.V. (2005): Microporous framework silicate minerals with rare and transition elements: minerogenetic aspects. *in* ''Micro- and Mesoporous Mineral Phases''. *Rev. Mineral. Geochem.,* **57**, 145–171.

Pyatenko, Yu.A., Kurova, T.A., Chernitsova, N.M., Pudovkina, Z.V., Blinov, V.A., Maksimova, N.V. (1999): Niobium, Tantalum and Zirconium in Minerals. IMGRE Publishing, Moscow, 213 p. (in Russian).

Sandomirsky, P.A. & Belov, N.V. (1984): Crystal Chemistry of Mixed Anionic Radicals. Nauka Publishing, Moscow, 205 p. (in Russian).

Saxton, R.J. (1999): Crystalline microporous titanium silicates. *Topics Catal.*, **9**, 43–57.

Sheldrick, G.M. (2008): A short history of SHELX. *Acta Crystallogr.,* **A64**, 112–122.

Valtchev, V., Paillaud, J.L., Mintova, S., Kessler, H. (1999): Investigation of the ion-exchanged forms of the microporous titanosilicate $K_2TiSi_3O_9 \cdot H_2O$. *Micropor. Mesopor. Mater.*, **32**, 287–296.

Zak, S.I., Kamenev, E.A., Minakov, F.V., Armand, A.L., Mikheichev, A.S., Petersil'e, I.A. (1972): The Khibiny Alkaline Massif. Nedra, Leningrad, 175 p. (in Russian).

Zou, X., Dadachov, M.S. (2000): $K_2TiSi_3O_9 \cdot H_2O$. *Acta Crystallogr.*, **C56**, 738–739.